A Demonstration of Self Organised Criticality: The Oslo Model

Shona Curtis-Walcott

Word Count: 2494

Abstract

An investigation into the Oslo Model was undertaken as means of exploring Self Organised Criticality, a property inherent to all dynamical systems with a steady state attractor. The model details a pile of rice onto which grains are added and avalanches spanning many orders of magnitudes are observed. Properties of the model were examined, namely the heights of grain piles, cross-over times, corrections to scaling, and avalanche size probability distributions, each for a range of system size $L \in \{4, 8, 16, 32, 64, 128, 256\}$. A finite scaling ansatz is deduced to support corrections to scaling observed in the average heights and slopes of the systems. The scaling parameters τ_s and D were identified via both data collapse and moment analysis. The moment analysis returned final values $D = 2.220 \pm 0.0019$ and $\tau_s = 1.550 \pm 0.058$.

I. Introduction

Complex systems theory strives to address how global phenomena arise from local interactions between the many small components of a dynamical system. It provides an explanation for phenomena which fail to be described using classical laws, an example of which is the Bak-Sneppen model which concerns the co-evolution of two species [1].

The Oslo Model is a generalisation of the one dimensional Bak-Tang-Wiesenfeld (BTW) model, introduced by Per Bak, Chao Tang and Kurt Wiesenfeld in their 1987 paper [2]. The BTW model was the first example of a critical system which displayed Self Organised Criticality (SOC). The central characteristic of SOC is the self-organisation of a system into a steady state configuration following a system disturbance. No external fine-tuning of relevant parameters is required for the system to converge to this stead state; the reaction of the system to a perturbation is independent of the perturbation itself. A further property of SOC is that it is scale invariant, and as such, a range of system sizes are to be considered in the Oslo Model simulated in this investigation.

II. The Oslo Model

A. Implementation

The Oslo model takes the form of a 1D lattice of size L onto which 'rice grains' are added to the first site (i =*1*) one by one. The lattice builds up and experiences avalanches in a stochastic manner: only when the slope at site *i*, z_i, is of greater value than the threshold slope z_i^{thresh} will a relaxation of grains to neighbouring sites occur. To initialise the threshold slopes an array of length L is randomly assigned values of 1 or 2 using a pseudo number generator. After each grain addition the slope at every site $i \in \{1, 2, 3...L\}$ is checked against its assigned threshold slope; if a relaxation has occurred the site will be assigned a new threshold slope according to the following probability:

$$z_i^{thresh} = \begin{cases} 1 & \text{with probability } p. \\ 2 & \text{with probability } \textit{1-p}. \end{cases} \tag{1}$$

B. Preliminary Testing of Model

When *p*=1 the Oslo model becomes identical to the original BTW model. A snapshot in time of the system configuration once a system of size $L = 100$ has reached a steady state is displayed in Fig. 1. A clear characteristic of the BTW model is the right angle triangle formed in the steady state with $z_i = 1 \forall i$. The first pile has a height equal to that of the system size, $h_{i=1} = L$.

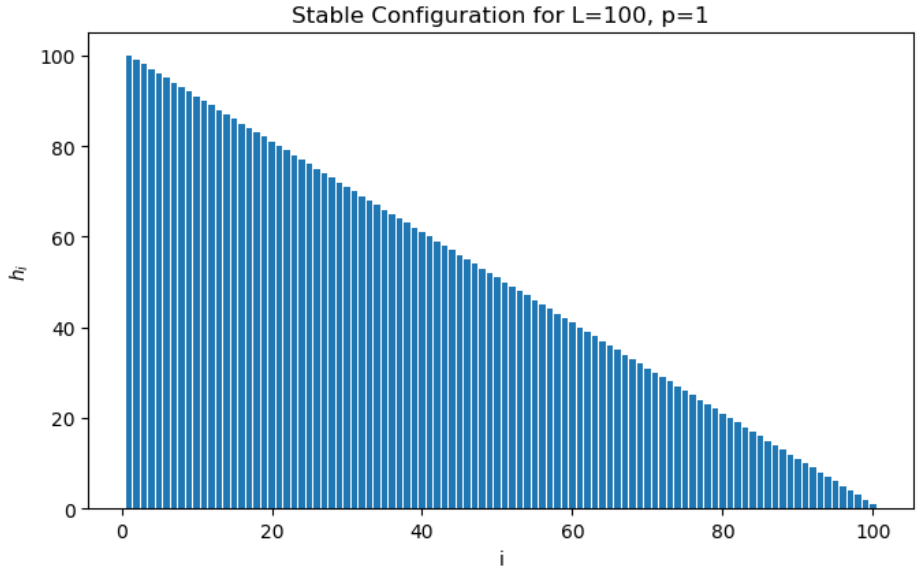

Fig. 1: The steady state configuration of the Oslo Model with $p = 1$ for a system of size $L = 100$, where h_i is the height of the i^{th} pile. Under these conditions the Oslo model is identical to the BTW model.

As the expected steady state height and crossover time for the BTW model are simple to calculate, they can be compared with measured values as means of a preliminary test. Note that in addition to the Oslo Model resembling the BTW Model when *p*=1, when *p*=0 it resembles the BTW model with double the original threshold slope. One can further expect the measured data for *p*=0.5 to lie between that collected for *p*=0 and *p*=1.

	Steady State Height		Cross-Over Time	
	Expected	Measured	Expected	Measured
p=1	100	100.0	5050	5050.0
p=$\frac{1}{2}$	$100 < h < 10100$	171.0	$5050 < t < 10100$	8645.0
p=0	200	200.0	10100	10100

TABLE I: The Oslo model simulation is tested using a comparison of expected vs. measured values for the steady state height of the system and the cross-over time. A system of $L = 100$ is used with a total of 200,000 grains added to the system.

The values returned by the model match predictions and indicate the code is working as intended.

III. System Height

The system height $h(t; L)$ is defined as the number of grains at site *i*=1 of the rice pile. Systems of size $L \in \{4, 8, 16, 32, 64, 128, 256\}$ are investigated and time is measured in units of grains

added to the system.

A. Transient and Recurrent Configurations

To display Self-Organised Criticality it is expected that a system will adopt a series of transient configurations followed by a set of recurrent configurations. The system height $h(t;L)$ should therefore be seen to increase as grains are added to the system and eventually level-off to a height $\langle h(t;L)\rangle_t$ once a steady state is reached. This behaviour is visible in Fig. 2 where the same trend is followed for all system sizes: $h(t;L)$ increases at a decreasing rate, then fluctuates around the steady state height $\langle h(t;L)\rangle_t$ indefinitely. The system follows the behaviour predicted for a self-organising system.

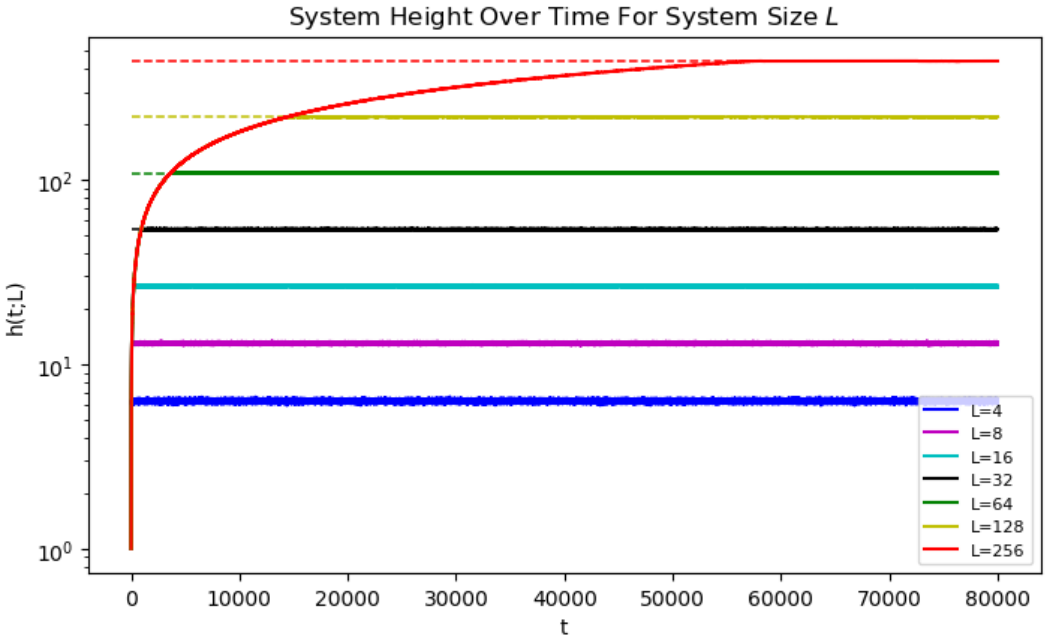

Fig. 2: The Oslo model was run 80,000 times with 100 repetitions per iteration, allowing for the averaging of collected data. The height $h(t;L)$ of site *i*=1 of the rice pile is plotted against time for system sizes $L \in \{4, 8, 16, 32, 64, 128, 256\}$ on a logarithmic scale, where time t is defined as the number of grains added to the system. The dashed lines indicate the steady state heights to which the system converges, $h_{av}(t;L) = 6.311, 12.980, 26.528, 53.887, 108.895, 219.289, 440.427$ for the system sizes L respectively.

B. Theoretical Justification

The height of a rice pile can be expressed both in terms of the slope value at each site $z_i(t)$, and the position-averaged slope $\langle z_i(t;L)\rangle$:

$$h(t;L) = \sum_{i=1}^{L} z_i(t) = L\frac{1}{L}\sum_{i=1}^{L} z_i(t) = L\langle z_i(t;L)\rangle. \tag{2}$$

The steady state is defined as the point at which the average influx of grains to the system is equal to the outflux; once reached there will be a constant number of grains in the system at

any one time. As z_i^{thresh} can only take one of two set values, the average slope of the system $\langle z \rangle$ should tend to a constant $\langle z_i(t;L) \rangle \approx \langle z \rangle$ when the steady state is reached. Substituting this into Eq. (2) it can be postulated that for large L the height of a pile scales as:

$$h(t;L) \approx L\langle z \rangle. \tag{3}$$

The cross-over time $\langle t_c(L) \rangle$ is defined as the time at which a grain first leaves the system (i.e. relaxes from site $i = L$). Having seen that a rice pile formation tends to an approximate right-angled triangle in the steady state, it can be estimated that the number of grains in a system of size L is simply $\frac{1}{2}Lh(t;L)$ for $L >> 1$. Furthermore, as time is measured in grain units, this grain number estimation can be substituted into Eq. (3) leading to an expression for the average cross-over time for $L >> 1$,

$$\langle t_c(L) \rangle = \frac{L^2\langle z \rangle}{2}. \tag{4}$$

C. Data Collapse for Processed Height

With the gathered knowledge of the system height having an approximately linear dependence on L (Eq. (3)) and the cross-over time having a quadratic dependence on L (Eq. (4)), a dimensionless scaling function $\mathcal{F}$ can be defined such that,

$$\tilde{h}(t;L) = L\mathcal{F}\left(\frac{t}{L^2}\right) \tag{5}$$

where,

$$\mathcal{F}(v) = \begin{cases} 0 & \text{for } v = 0. \\ \langle z \rangle & \text{for } v \geqslant 1 \end{cases} \tag{6}$$

where $\mathcal{F}$ is expected to be a linearly increasing function between $v = 0$ and $v \backsim 1$. A data collapse of system height is created by plotting $\frac{\tilde{h}(t;L)}{L}$ against $\frac{t}{L^2}$, displayed in Fig. 3. The trend observed matches that expected from the proposed scaling function $\mathcal{F}(v)$, where v is seen to be a number just less than 1. The collapsed plots do not lie directly on top of one another, shown in Fig. 4, owing to corrections to scaling as the defect is visibly worse for smaller system sizes.

The gradient of the linear region for system size $L = 256$ is measured as 0.5968 ± 0.0004 indicating the following, where $c \leqslant 1$.

$$\mathcal{F}(v) = v^{0.597} \text{ for } 0 \leqslant v \leqslant c \tag{7}$$

D. Cross-Over Time Scaling

The number of grains in the system at any time is given by $N = \sum_{i=1}^{N} iz_i$, from which an expression for the cross-over time can be developed:

$$t_c(L) = \sum_{i=1}^{L} iz_i = L\frac{1}{L}\sum_{i=1}^{L} iz_i = L\langle iz_i(L) \rangle. \tag{8}$$

Since $\langle AB \rangle = \langle A \rangle \langle B \rangle$, the right hand side of Eq. (8) can be expanded:

$$L\langle z_i(L) \rangle \langle i \rangle = L\langle z_i(L) \rangle \frac{1}{L}\sum_{i=1}^{L} i = \langle z_i(L) \rangle \frac{L(L+1)}{2L} \tag{9}$$

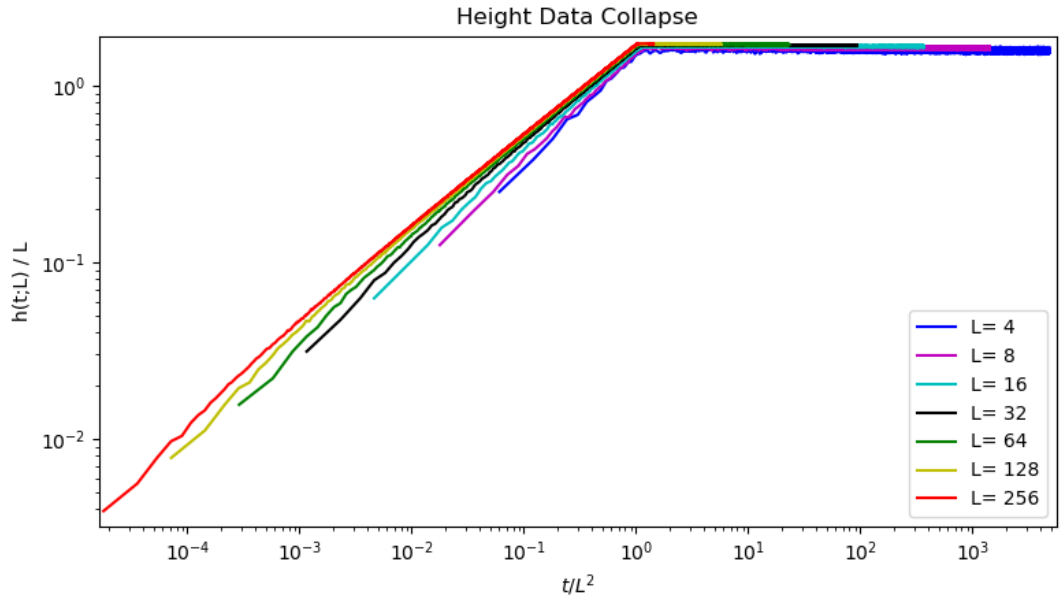

Fig. 3: A data collapse of $\frac{h(t;L)}{L}$ against $\frac{t}{L^2}$ for various system sizes $L \in \{4, 8, 16, 32, 64, 128, 256\}$, displayed on a logarithmic scale. The slope of the linear region is measured for system size $L = 256$ as it experiences the largest number of transient states, returning 0.5968 ± 0.0004.

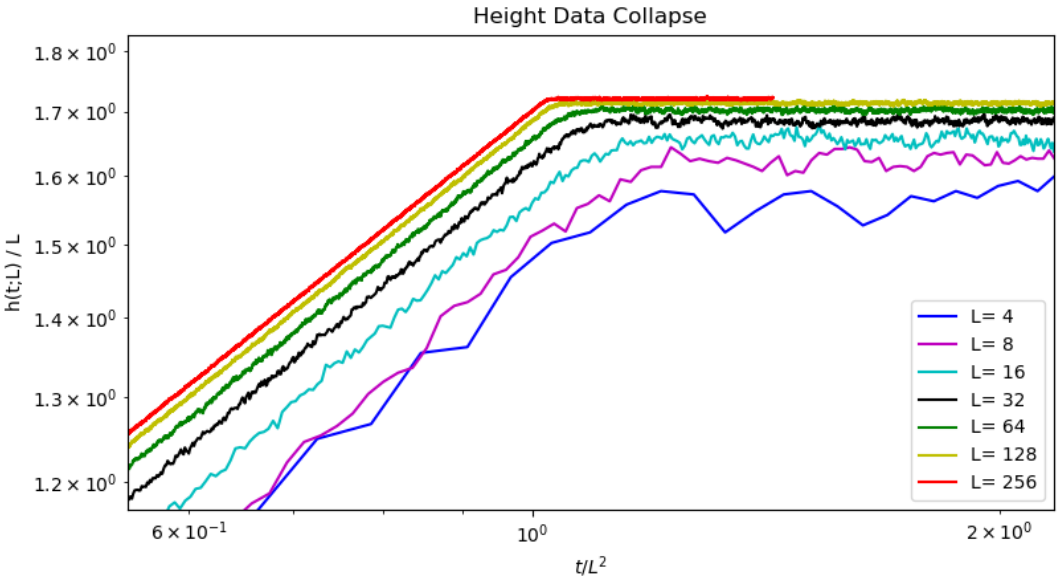

Fig. 4: An enlarged version of Fig. 3 which reveals defects present for small system sizes induced by corrections to scaling. As all plots collapse towards that of the largest system size, $L = 256$, it can be expected for much larger system sizes that performing a data collapse should stack each plot on top of one another.

leading to,

$$t_c(L) = \frac{\langle z_i(L) \rangle}{2} L^2 \left(1 + \frac{1}{L}\right). \tag{10}$$

As all dynamics displayed by the model so far have shown consistency with SOC, it can be assumed that the cross-over time will not depend on the system size L and Eq. (10) can be re-expressed:

$$\langle t_c(L)\rangle = \frac{\langle z\rangle}{2} L^2 \left(1 + \frac{1}{L}\right). \tag{11}$$

Two estimates for $\langle z\rangle$ were collected: the first, $\langle z\rangle_0$, was measured as the average slope of the system at the first instance of a grain leaving the system. Although the system is expected to have reached a steady state by the time $\langle z\rangle_0$ is measured, there is a chance the configuration may not belong to the set of recurrent configurations between which the system will fluctuate as $t \to \infty$. A second $\langle z\rangle$ is therefore calculated as the mean of measured average system slopes over the course of 1000 grain additions at large t, $\langle z\rangle_{ext}$. Both estimates are used in Eq. (11) to calculate estimates for the theoretical crossover time.

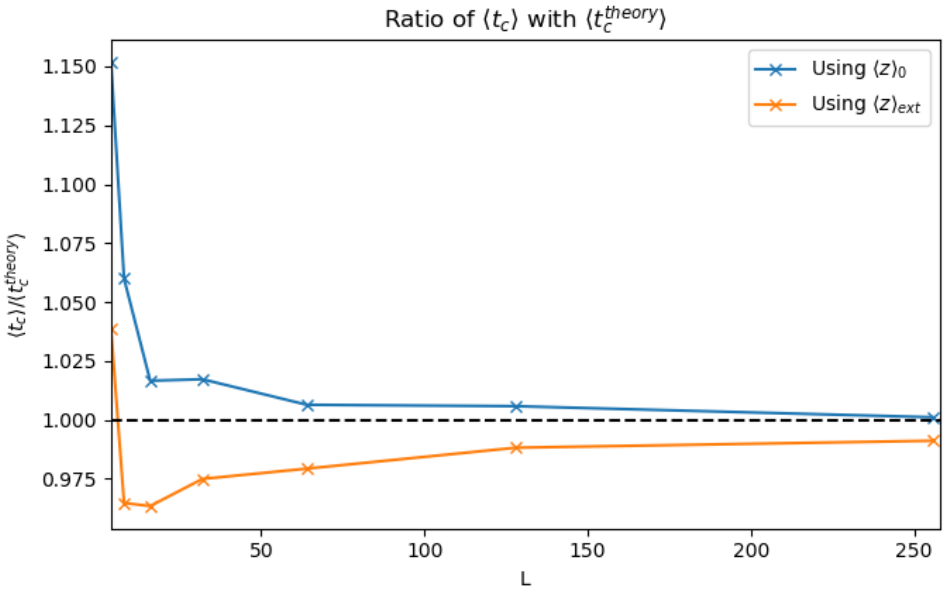

Fig. 5: Plot of the ratio between measured cross-over times $\langle t_c\rangle$ and estimates for the theoretical cross-over time $\langle t_c^{theory}\rangle$. $\langle t_c^{theory}\rangle$ was calculated through Eq. (11) using two estimates of the average slope of the system $\langle z\rangle$: the first, $\langle z\rangle_0$, was measured at the first instance of a grain leaving the system, and the second, $\langle z\rangle_{ext}$, was taken as an mean of average slopes recorded further into the steady state of the system.

In Fig. 5 a significant deviation of both ratios from theory is seen for small L values, owing to the large corrections to scaling present. Although both methods of calculating $\langle t_c^{theory}\rangle$ show the measured $\langle t_c\rangle$ values do tend to theoretical expectation, the theoretical crossover times calculated using $\langle z\rangle_0$ match the measured data more and hence displays a faster convergence. The two methods only converge in the limit $L \to \infty$ indicating that for small L, $\langle z_i(t;L)\rangle \not\approx \langle z\rangle$. As this report deals only with finite system sizes, in all further calculations $\langle z\rangle_0$ is used for $\langle z\rangle$.

E. Corrections To Scaling

Although Eq. (3) holds in the limit of large L, it has been shown that corrections to scaling are required for systems of finite size. When considering first order corrections to scaling, the

steady state height of the system $\langle h(L)\rangle_t$ becomes [3],

$$\langle h(L)\rangle_t = a_0 L(1 - a_1 L^{-\omega_1}) \tag{12}$$

which can be re-expressed as,

$$log\Big(1 - \frac{\langle h(L)\rangle_t}{a_0 L}\Big) = -\omega_1 log(L) + log(a_1) \tag{13}$$

and so plot of $log\Big(1 - \frac{\langle h(L)\rangle_t}{a_0 L}\Big)$ against $log(L)$ is expected to produce a straight line graph with gradient $-\omega_1$. In the limit of $L \to \infty$ Eq. (12) must tend to Eq. (3) and therefore $\langle z\rangle = a_0$.

The Oslo Model was run once over 5000,000 iterations for each system size. The heights of the system for the last 4000,000 iterations are analysed to ensure only steady state results are considered. Values for $\langle h(L)\rangle_t$ are calculated by taking the mean of measured system heights, and the results are plotted against L in Fig. 6 to get an estimate for a_0 as per Eq. (3). The slope, $a_0 = 1.727$, was only measured between $L = 64$ and 256 as Eq. (3) holds only for large L. This estimate was used in Eq. (13) to produce Fig. 7, however the expected linear trend is not seen. This confirms the existence of corrections to scaling as without them this initial estimate would have produced a linear fit.

The parameter a_0 is therefore optimised: numbers either side of 1.727 are tested and a minimisation of the sum of squared residuals (SSR) is performed. This returns an improved estimate of $a_0 = 1.739 \pm 0.01$ where the error is calculated as the difference between the best estimate of a_0 and the value of a_0 which returned the next-best residual in the optimisation process. The updated fit of Eq. (13) is plotted in Fig. 8 and returns values of $\omega_1 = 0.530 \pm 0.032$ and $a_1 = 0.198 \pm 0.013$.

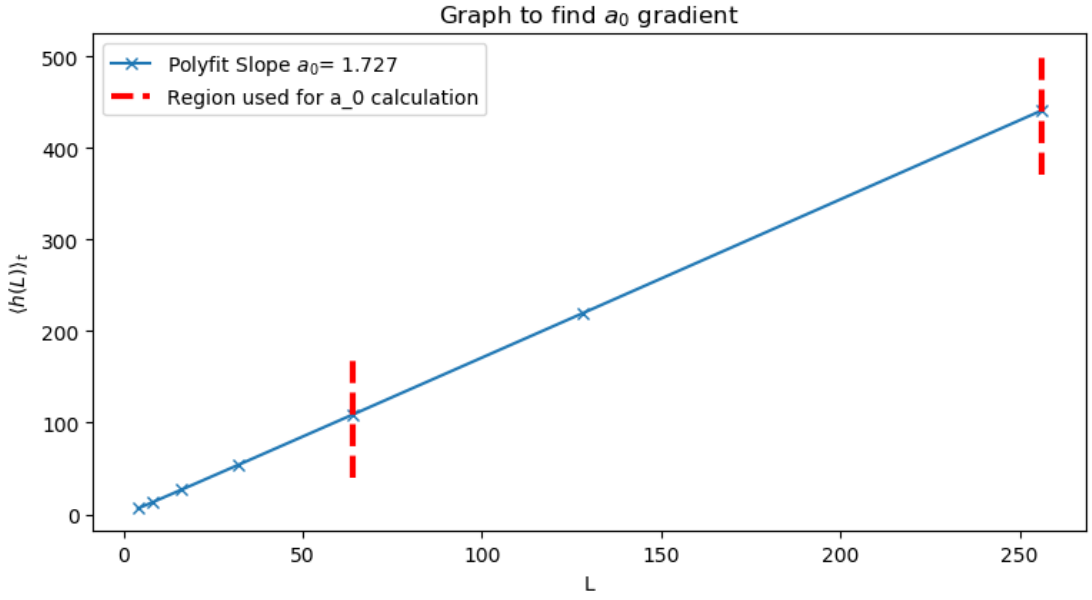

Fig. 6: Average system height $\langle h(L)\rangle_t$ is plotted against system size L. The slope is measured between points $L = 64$ and $L = 256$ as Eq. (3) holds only in the limit of large L. The slope, a_0, is found to be 1.727.

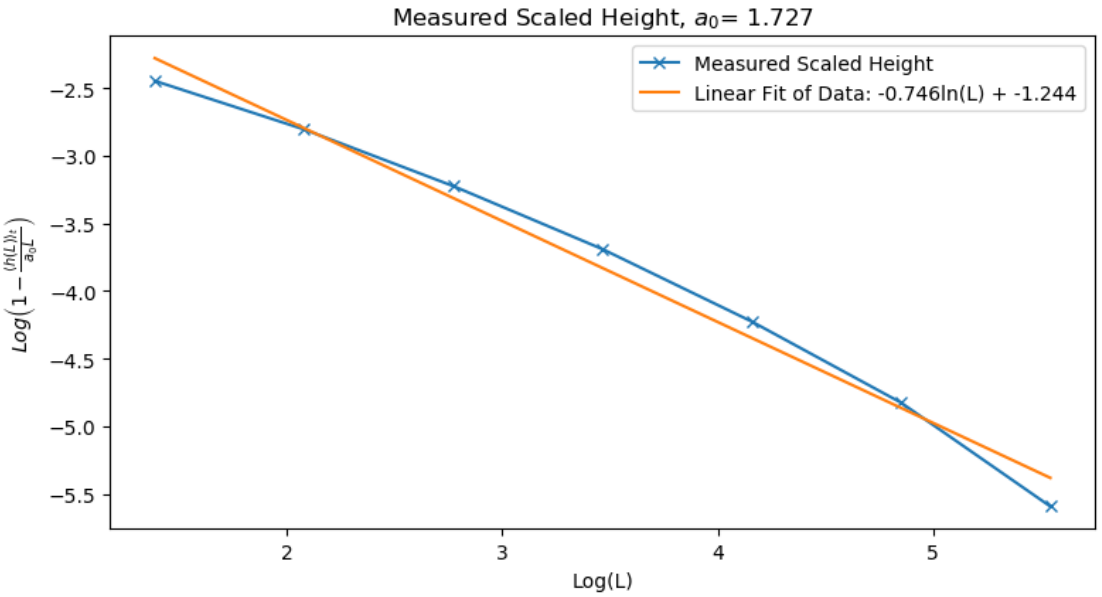

Fig. 7: Plot of the scaled height $log\left(1-\frac{\langle h(L)\rangle_t}{a_0 L}\right)$ against $log(L)$ using the estimated parameter value of $a_0 = 1.727$ where the scaled measured data is plotted in blue, and the linear fit is plotted in orange. This estimated value of a_0, found through Eq. (3), returns a poor sum of squared residuals (SSR) value of 0.4 and estimates $\omega_1 = 0.53 \pm 0.032$. Therefore an optimisation for a_0 must be performed.

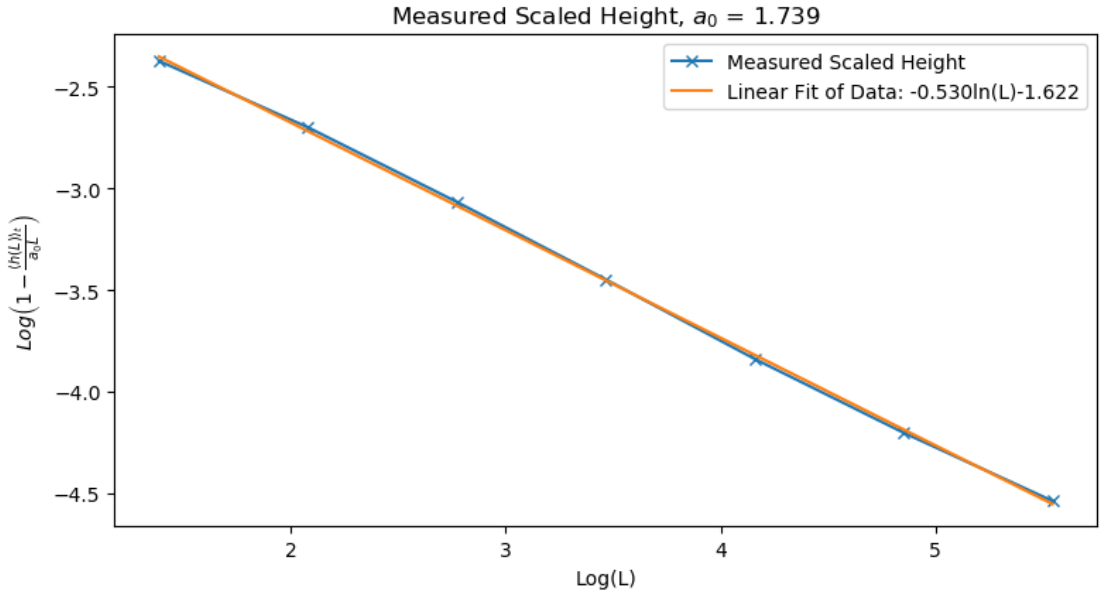

Fig. 8: Using the updated estimate $a_0 = 1.739 \pm 0.01$ found via SSR minimisation, a linear fit to the scaled measured data is seen. Updated corrections to scaling estimates of $\omega_1 = 0.530 \pm 0.032$ and $a_1 = 0.198 \pm 0.013$ are returned. The updated estimate for scaled measured data is indicated in blue, and the linear fit is in orange.

F. Statistical Fluctuations

From Eq. (3), one can express the position-averaged slope as

$$\langle z(L)\rangle = \frac{\langle h(t;L)\rangle}{L}. \tag{14}$$

Given L refers to a parameter and not statistics, it has no standard deviation. The standard deviation of the position-averaged slope, $\sigma_{\langle z\rangle}(L)$, can therefore be expressed simply in terms of the standard deviation of system height from its average value at steady state, $\sigma_h(L)$:

$$\sigma_{\langle z\rangle}(L) = \frac{\sigma_h(L)}{L}. \tag{15}$$

The standard deviation $\sigma_h(L)$ is calculated from collected data and plotted against system size L on a logarithmic scale, seen in Fig. 9. For the smallest value of L a slight deviation of measured data from the linear fit can be seen, owing to corrections to scaling.

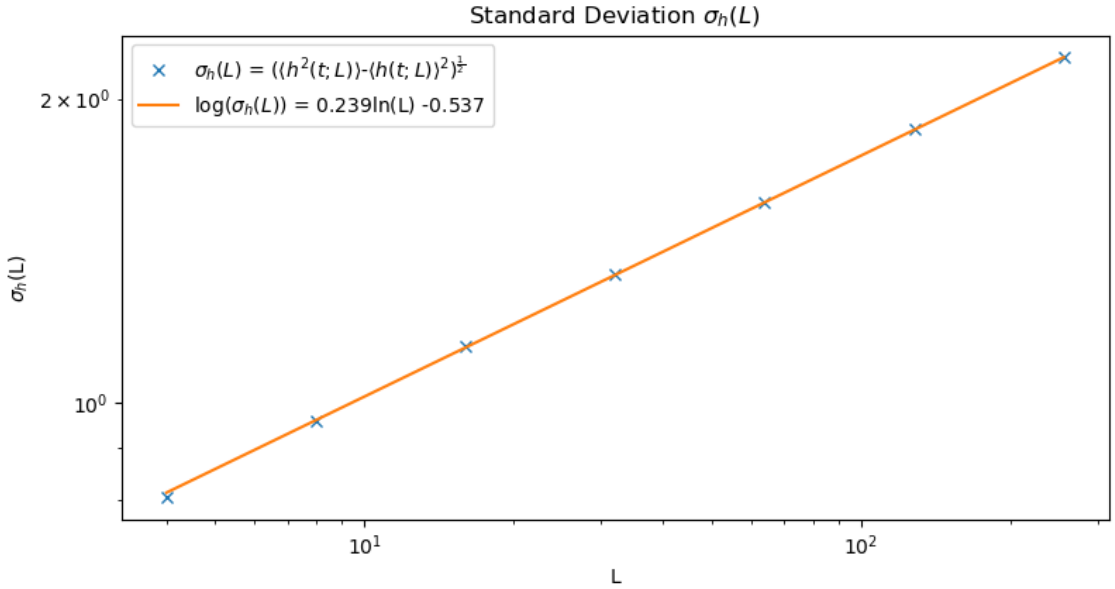

Fig. 9: The position-averaged slope, $\sigma_{\langle z\rangle}(L)$ is plotted against system size L on a logarithmic scale. A linear fit is plotted of gradient 0.239 ± 0.002.

From the slope in Fig. 9, it is found that $\sigma_h(L) \approx L^{0.239\pm0.002}$ with a small SSR of 10^{-5}. From Eq. (15) it can now be predicted that,

$$\sigma_{\langle z\rangle}(L) = \frac{\sigma_h(L)}{L}. \sim \frac{L^{0.239\pm0.002}}{L} = \frac{1}{L^{0.761\pm0.002}} \tag{16}$$

This power law relationship is in fact seen in Fig. 10, where $\sigma_{\langle z\rangle}(L) = L^{-0.761\pm0.002}$ contains the observed power law within its uncertainty range. It can now be predicted that as $L \to \infty$, $\sigma_z(L)$ will tend to zero and $\langle z\rangle$ will tend to a_0 as per Eq. (14).

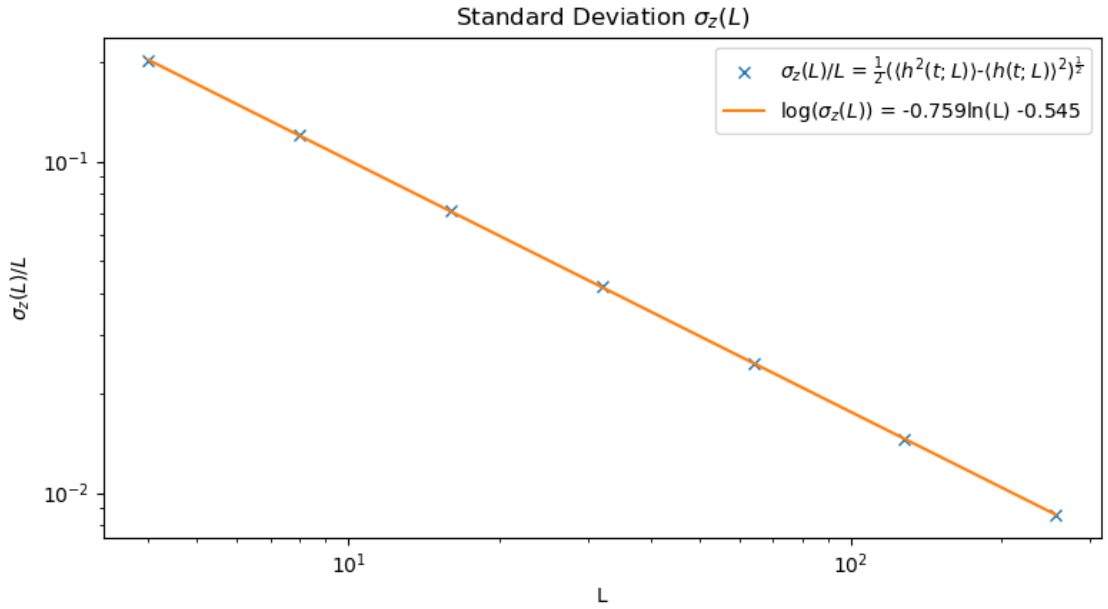

Fig. 10: The position-averaged slope, $\sigma_{\langle z\rangle}(L)$, is scaled with system size L and plotted against L on a logarithmic scale. The linear fit returns a slope of -0.759 ± 0.002.

G. Height Probability Distribution

If the assumption is made that z_i are independent and identically distributed random variables, then the standard deviation $\sigma_{\langle z\rangle}$ can be expressed,

$$\sigma_{\langle z\rangle}(L) = \sqrt{\frac{1}{L-1}\sum_{i=1}^{L}(z-\bar{z})^2} \sim \frac{1}{\sqrt{L}} \tag{17}$$

which holds in the limit of large L and indicates that the time-averaged height data should scale as,

$$\sigma_h = L\sigma_z(L) \sim \sqrt{L}. \tag{18}$$

As system height is described by a sum of the individual slopes z_i (Eq (2)) from the Central Limit Theorem it is expected that the probability distribution of height data will take a Gaussian form with standard deviation $\sigma_h \sim L^{-\frac{1}{2}}$ and peak height $h_{peak} = \langle h(L)\rangle_t$. The height probabilities are displayed in Fig. 11.

A data collapse is implemented by plotting $P(h;L)\sigma_h$ against $\frac{h-\langle h(t;L)\rangle_t}{\sigma_h}$, alongside a normalised Gaussian of parameter values $\sigma_G = 1$, $\mu_G = 0$, displayed in Fig.12. As all data collapses onto the same single distribution it can be deduced that the height distributions of the system tends to same state. This is a feature of a self-organising system. Although a scaling of $\sigma_h \sim L^{-\frac{1}{2}}$ was predicted by theory, it was previously shown (Fig. 10) that the measured σ_h actually follow a power law $\approx L^{-0.759}$. The discrepancy is a result of the false assumption that z_i are independent variables; false as in this model there exist different relaxation conditions near the system boundary sites $i = 0$ and $i = L$ compared to the central sites of the system. The data collapse reveals a distinct positive skewness in the measured data and indicates larger system sizes L produce more Gaussian-like probability distributions which is as predicted by the Central Limit Theorem. In the limit of $L \to \infty$, avalanches of an infinitely large sizes are possible and hence systems will have a infinitely varying height. Therefore σ_h will also tend to infinity.

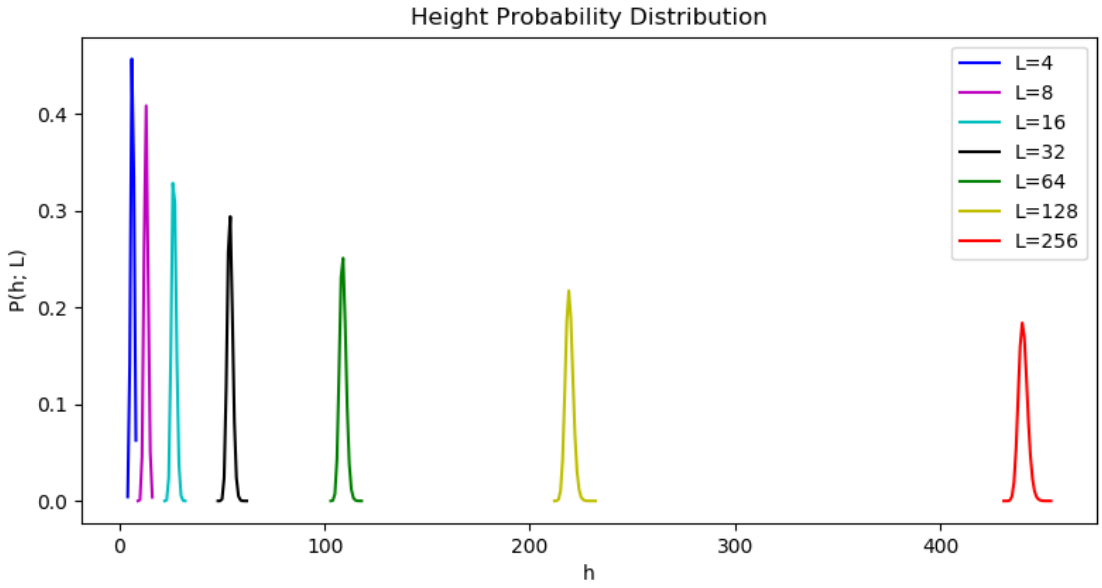

Fig. 11: The height probability distribution $P(h;L)$ displayed for all system sizes. The individual distributions show a roughly Gaussian structure as predicted.

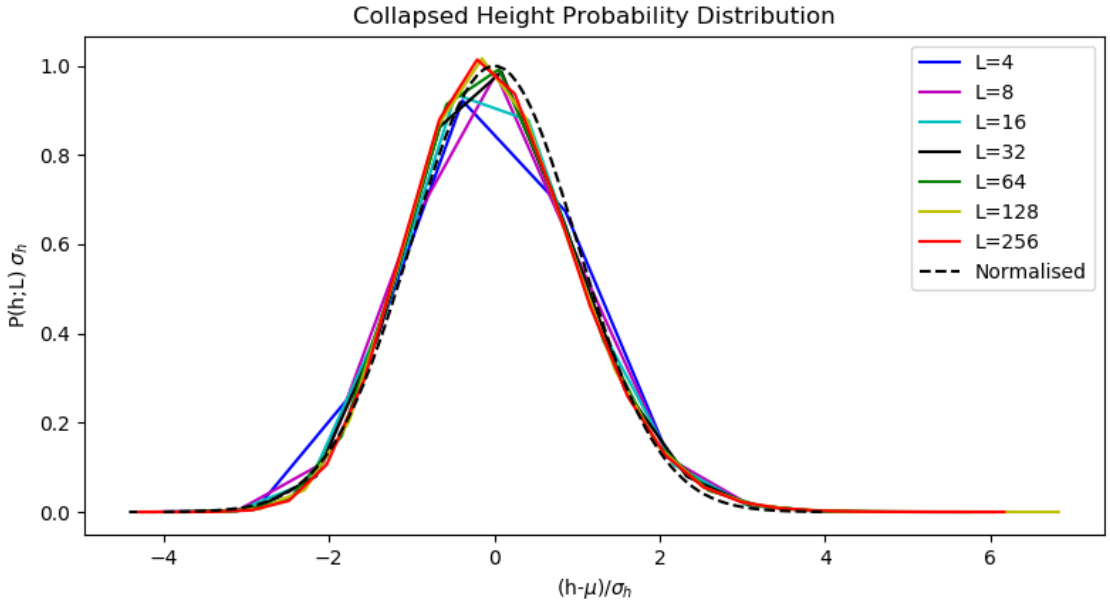

Fig. 12: A data collapse of the height probability distribution $P(h;L)$ is plotted as $P(h;L)\sigma_h$ against $\frac{h-\langle h(t;L)\rangle_t}{\sigma_h}$. A normalised Gaussian has also been plotted and reveals a positive skewness in the data.

IV. Avalanche Sizes

A. *Avalanche Size Probability Distribution*

In the Oslo Model, the size of an avalanche s is defined as the number of site relaxations induced by a single grain addition to the system, where the probability of an avalanche of size

s being induced is,

$$P_N(s;L) = \frac{\text{No. of avalanches of size s in a system of size L}}{\text{Total no. of avalanches, N}}. \tag{19}$$

It is expected that $P_N(s;L)$ will decrease for increasing avalanche size, as each site relaxation requires $z_i > z_i^{thresh}$ and for a large avalanche numerous neighbouring sites must be in a state to satisfy this condition. To illustrate this, the normalised size of each induced avalanche for system of size $L = 128$ is plotted against time in Fig. 13, confirming that avalanche sizes over many orders of magnitude are induced and that large avalanches occur less frequently that small avalanches.

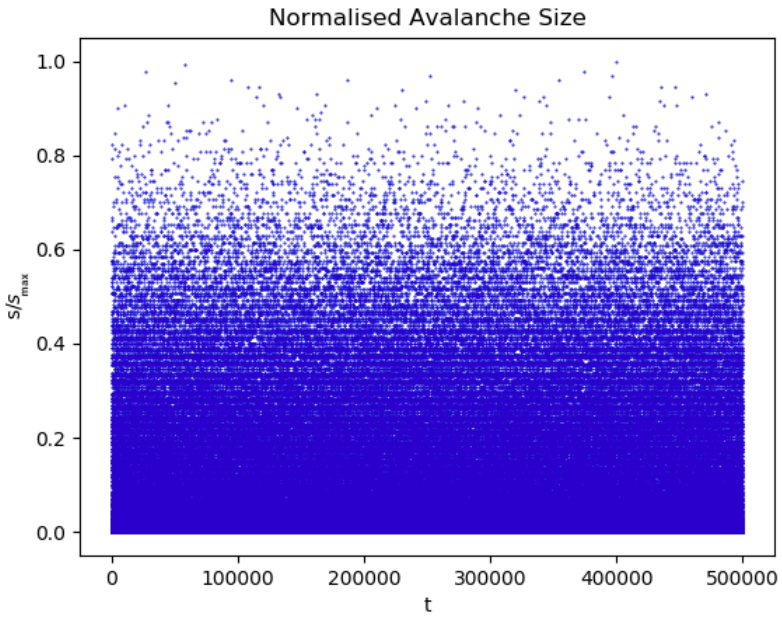

Fig. 13: Scatter graph of normalised avalanche size over time, where time is measured as the number of grains added to the system, for system size $L = 128$ with $5000,000$ grain additions. The measured avalanche sizes are observed to span many orders of magnitude.

A characteristic of SOC is that for a system of size L there is a maximum avalanche size s_M which can be induced by any grain addition. As seen in Fig. 14 the data near s_M contains a disproportionate amount of noise. To combat this a log-binning function is applied to the data to extract the useful information. Fig. 15 displays $\tilde{P}(s^j;L)$: the probability that an avalanche size belongs the j^{th} bin of the plot, where the bins are logarithmically spaced so each bin is a factor of 1.25 times larger than the previous. This chosen scale of 1.25 is a compromise between the loss of less information subject at small scales, and the increased cleanliness of data subject at large scales.

Fig. 15 displays a clear trend across all system sizes as an asymptote followed by a bump and decrease of $\tilde{P}(s^j;L)$ with s. The peak in $\tilde{P}(s^j;L)$ for $s < s_M$ owes to the finite size of systems considered in this model; the size of the largest avalanches for each system are capped by the value of s_M and therefore a build-up of avalanche occurs in the vicinity of s_M. Observing the trend for the largest system size suggests that data collected for a system of infinite size would simply continue along the linear trend.

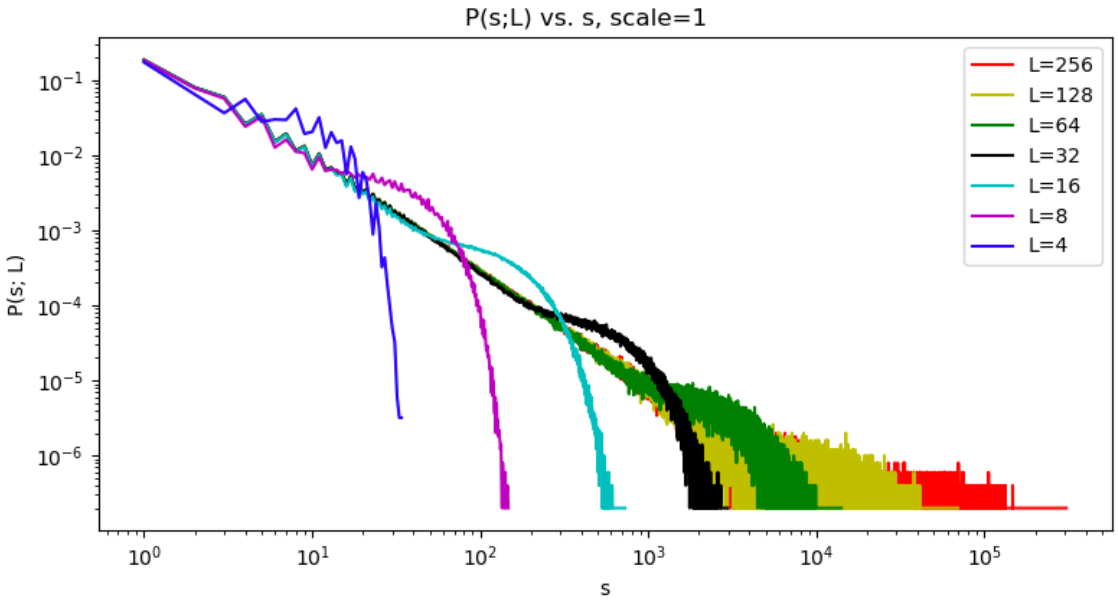

Fig. 14: The avalanche size probability distribution has been log-binned and plotted over all system sizes with linearly spaced bins. Avalanches of value zero have been omitted and the plot has a logarithmic scale. A total of 5000,000 grains have been added to each system.

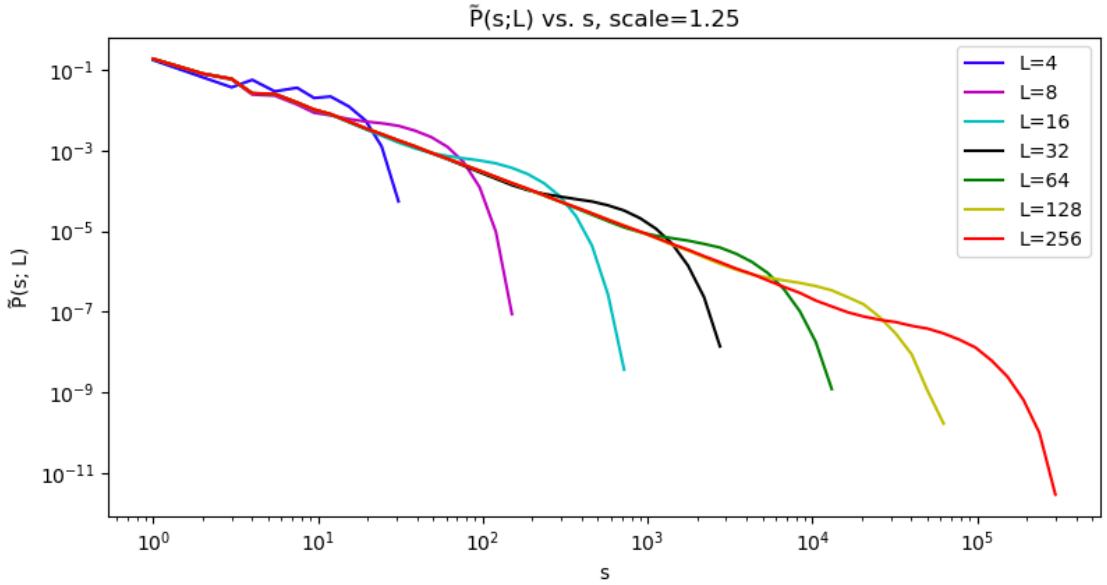

Fig. 15: The avalanche size probability distribution is plotted with logarithmically spaced bins of increasing size (scale of 1.25). Avalanches of size zero are once again omitted. The probability distribution of avalanche sizes is scale-invariant until $s \rightarrow s_M$.

B. Finite Scaling Ansatz

A finite scaling ansatz of the form

$$\tilde{P}(s^j; L) \propto s^{-\tau} \mathcal{G}\left(\frac{s}{s_M}\right) \tag{20}$$

is proposed for $L >> 1$ and $s >> 1$ [4].

The point at which $\tilde{P}(s^j; L)$ cuts off represents the largest avalanche which occurred for each system size; this is used as an estimate for s_M in Fig. 16 where s_M are plotted against L on a logarithmic scale. A power law between s_M and L is observed: $s_M = L^D$ for a constant D. The value of D is measured for the three largest system sizes, $L \in \{64, 128, 256\}$, returning $D = 2.254$.

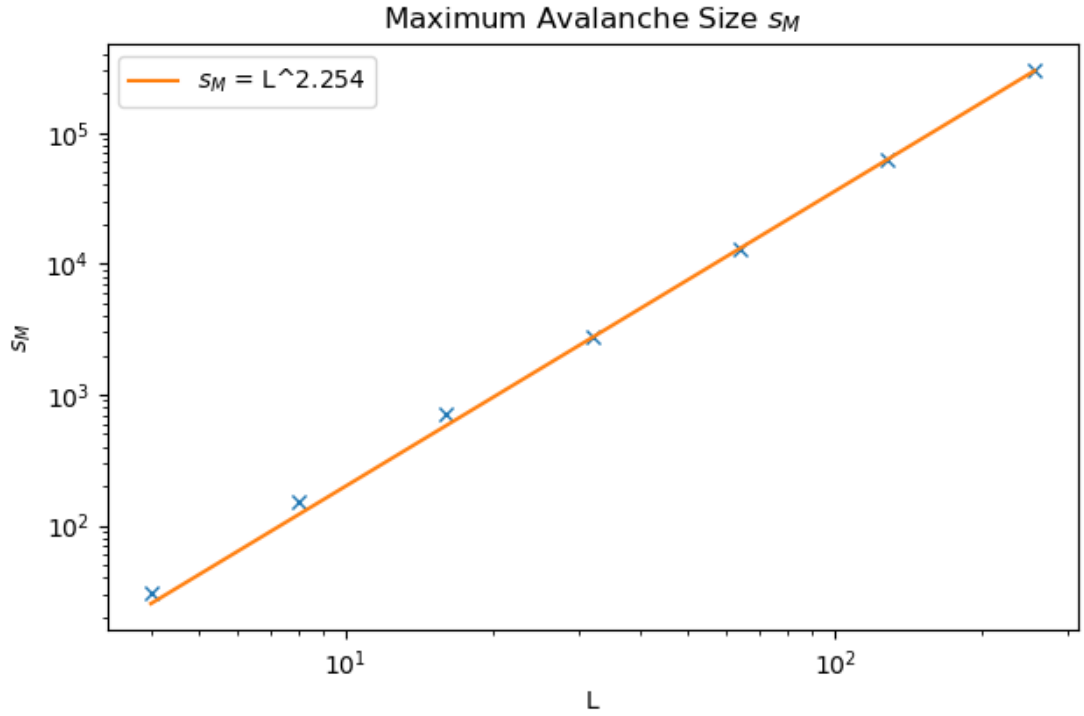

Fig. 16: Demonstration of the power law relationship betweens_M against L, plotted here on a logarithmic scale. The linear fit is fitted only for the three largest system sizes, $L \in \{64, 128, 256\}$, returning a gradient $D = 2.254$. The values of s_M have been taken as the avalanche size at which the lines in Fig. 15 terminate.

The linear section of Fig. 15 has a gradient τ_s which is measured for the largest system size $L = 256$ giving $\tau_s = -1.524 \pm 0.017$. Manipulation of Eq. (20) for the 0^{th} moment where probabilities sum to 1, returns the relation $D(2 - \tau_s) = 1$ from which the value of D can be estimated as $D = 2.100 \pm 0.017$.

The finite scaling ansatz can be verified by performing a data collapse $s^{\tau_s}\tilde{P}_N(s; L)$ against s/L^D, displayed in Fig. 17, where values of τ_s and D which align the data most effectively are $\tau_s = 1.530$ and $D = 2.140$.

C. *Moment Analysis*

Moment Scaling Analysis offers a further method through which the critical exponents D and τ_s can be calculated [5]. The k^{th} moment can be evaluated,

$$\langle s^k \rangle = \lim_{T\to\infty} \sum_{t=t_0+1}^{t_0+T} s_t^k \tag{21}$$

THE P() IS FROM DATA COLLAPSE
HOW DID I PLOT THAT AGAINST SMTH ELSE

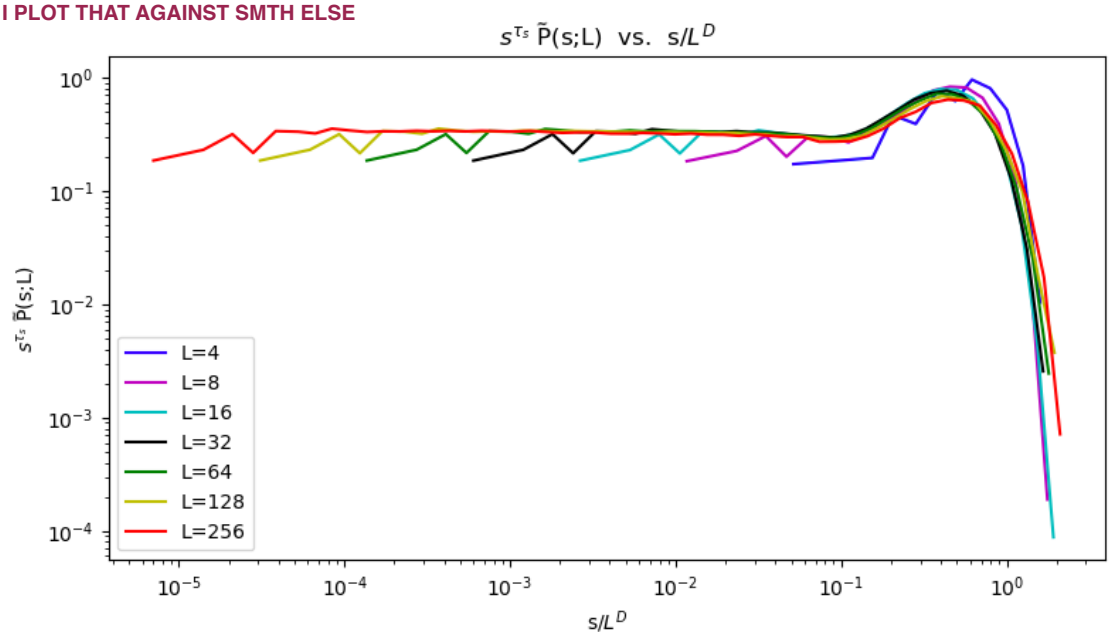

Fig. 17: The data collapse for avalanche size probability distribution is displayed with $s^{\tau_s}\tilde{P}_N(s;L)$ plotted against s/L^D where values of $\tau_s = 1.530$ and $D = 2.140$ are used to scale the axis.

where s_t is the measured avalanche size at time t. This can be re-expressed in terms of the avalanche size probability which can then be substituted for Eq. (20),

$$\langle s^k \rangle = \sum_{s=1}^{\infty} s^k P(s;L) = \sum_{s=1}^{\infty} s^{k-\tau_s} \mathcal{G}\left(\frac{s}{L^D}\right). \tag{22}$$

Now, approximating the right hand side of Eq. (22) as an integral, followed by a substitution of $v = \frac{s}{L^D}$,

$$\langle s^k \rangle \propto L^{D(1+k-\tau_s)} \int_{L^{-D}}^{\infty} v^{k-\tau_s} \mathcal{G} dv \tag{23}$$

For the integral to produce a number it must convergence at both limits: $\mathcal{G}$ can be seen to rapidly decay for large s values and hence the integral converges at the upper limit. In the limit of large L the lower limit tends to zero; the integral will converge here if $\tau_s = 1 + k$, i.e. if $v > -1$. Provided this is the case the integral does correspond to a constant value and the logarithm can be taken of both sides:

$$log(\langle s \rangle) = D(1 + k - \tau_s) + Constant. \tag{24}$$

This relation is plotted in Fig.18 for $k \in \{1, 2, 3, 4, 5, 6, 7, 8, 9\}$, where corrections to scaling are visible for low L values in the form of a deviation of measured points to the linear trend. These corrections arise due to having approximated the lower integral limit with zero; this only holds for large L values.

The slope of linear fits in Fig.18 are plotted against k in Fig.19, from which a value of $D = 2.200 \pm 0.019$ is found as $\frac{d}{dk} D(1 + k - \tau_s) = D$. An estimate of $\tau_s = 1.550 \pm 0.058$ can also be made as,

$$D(1 + k - \tau_s)\Big|_{k=\tau_s - 1} = 0. \tag{25}$$

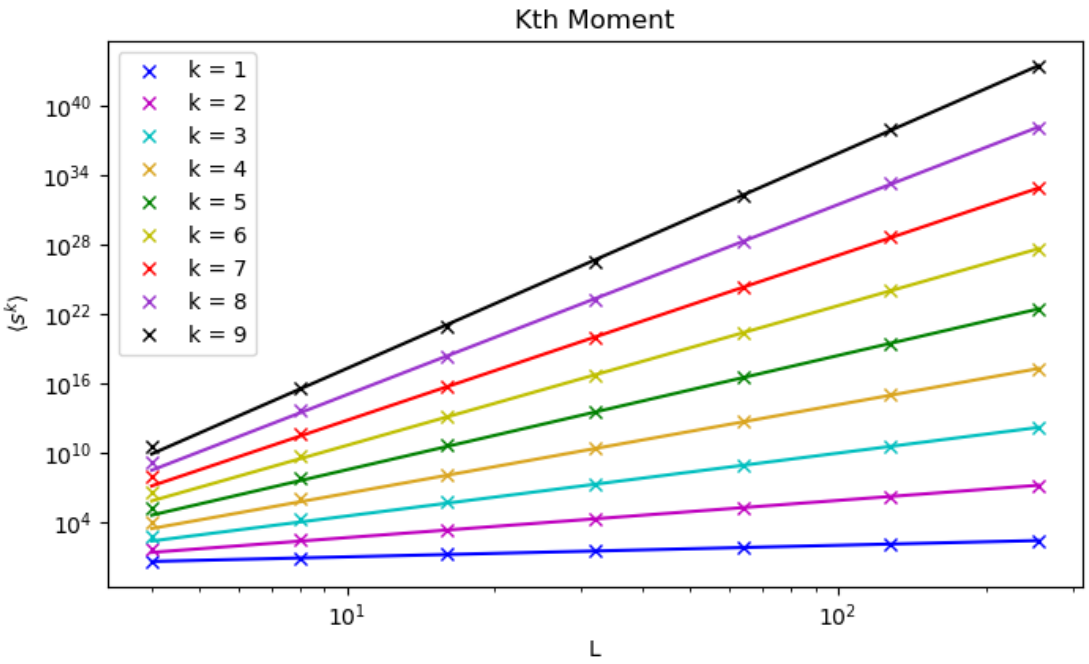

Fig. 18: A plot of the k^{th} moments $\langle s_k \rangle$ against system size for $k \in \{1, 2, 3, 4, 5, 6, 7, 8, 9\}$, displayed on a logarithmic scale. The linear plots are fitted for L values $\{64, 128, 256\}$ so as to highlight any potential corrections to scaling present at small L. A maximum SSR value of 0.075 arises in the linear fit for k=9.

Note that when measuring these slopes, only the five smallest values of k were considered as, given the power law stated in Eq. (21), a $\langle s^k \rangle$ measured with large k has a greater chance of being influenced by a random large measured avalanche sizes s_t, and is hence less stable.

These estimates of the critical exponents D and τ_s lie within 3.7% and 1.3% of the values which produced the best data collapse onto $\mathcal{G}$, and within 5.7% and 1.7% of those calculated from Fig. 15 and Eq. (20), respectively.

V. Conclusion

A computational program simulating the Oslo Model was written and tested for rice piles of size $L \in \{4, 8, 16, 32, 64, 128, 256\}$. Data was gathered on the average heights and slopes, as well as the height and avalanche size probability distributions observed as grains were added to the system. Corrections to scaling were also calculated where required. Each system was seen to go through transient states where the system height scaled as $h(t; L) \propto \sqrt{t}$, before stabilising at a steady state height without the need for external tuning.

A finite scaling ansatz for avalanche size probability was proven and the critical exponents of the avalanche size probability distribution were calculated via both a data collapse and a moment analysis. Performing a data collapse resulted in values of $D = 2.100 \pm 0.017$ and $\tau_s = 1.524 \pm 0.017$ while the moment analysis obtained $D = 2.220 \pm 0.0019$ and $\tau_s = 1.550 \pm 0.058$. The consistency of these results, along with the observed characteristics of the model discussed prove the simulated Oslo Model displayed self organising behaviour.

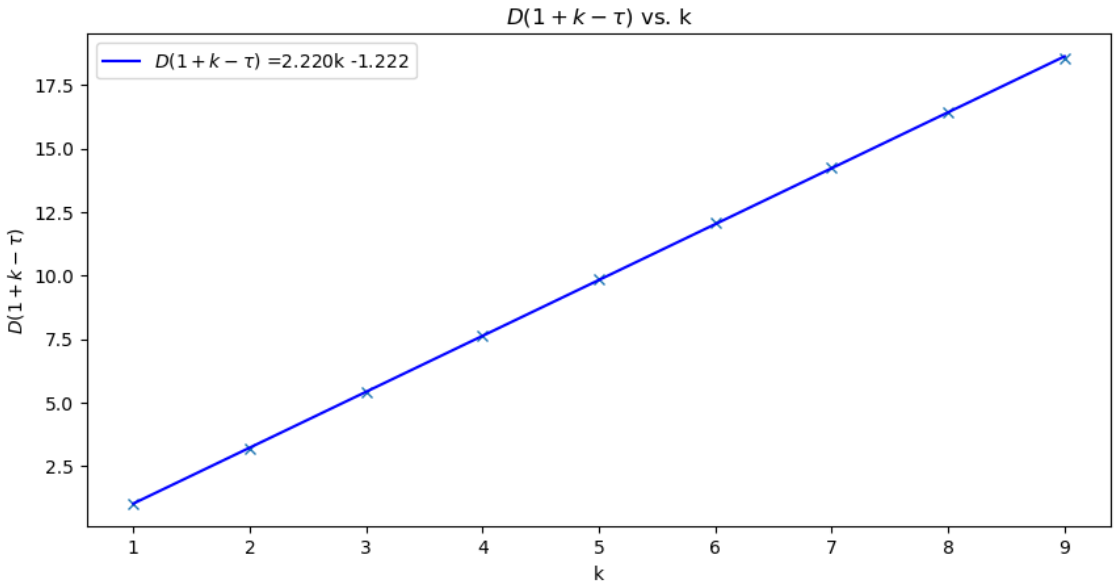

Fig. 19: The relation between $D(1+k-\tau_s)$ and k is plotted to allow for moment analysis. The linear fit is fitted for the first five k values and has a slope $D = 2.220 \pm 0.019$ which crosses the k-axis at $k = 0.550$. Using this information alongside Eq. (15) returns $\tau_s = 1.550 \pm 0.058$. No clear corrections to scaling are seen here, providing confidence in the returned critical exponent values.

REFERENCES

[1] N. R. Christensen, K.; Moloney, "*Punctuated equilibrium and criticality in a simple model of evolution*," vol. 71, no. 24, pp. 4083–4086, 1993.

[2] C. W. K. Bak, P.; Tang, "*Self-organized criticality: an explanation of 1/ noise* doi:10.1103," *Physical Review Letters.*, vol. 59, no. 4, p. 381–384, 1992.

[3] K.Christensen, *Chapter 3: Self Organised Criticality*, ser. From *Complexity project notes*, Centre for Complexity Science Imperial College London 2019.

[4] N. R. Christensen, K.; Moloney, "*Complexity and Criticality*," *Imperial College Press*, pp. 273–274, 2005.

[5] N. R. Christensen, K.; Moloney, "*Complexity and Criticality*," *Imperial College Press*, pp. 276–277, 2005.